Spectroscopy of betatron radiation emitted from laser-produced wakefield accelerated electrons[a)]

D. B. Thorn,[1,2] C. G. R. Geddes,[3] N. H. Matlis,[3] G. R. Plateau,[3,4] E. H. Esarey,[3] M. Battaglia,[3] C. B. Schroeder,[3] S. Shiraishi,[3] Th. Stöhlker,[2,5] C. Tóth,[3] and W. P. Leemans[3]
[1]*ExtreMe Matter Institute EMMI, 64291 Darmstadt, Germany*
[2]*GSI Helmholtzzentrum für Schwereionenforschung, 64291 Darmstadt, Germany*
[3]*Lawrence Berkeley National Laboratory, Berkeley, California 94720, USA*
[4]*École Polytechnique, 91128 Palaiseau, France*
[5]*Helmholtz Institute Jena, 07743 Jena, Germany*

(Presented 19 May 2010; received 15 May 2010; accepted 8 July 2010; published online 28 October 2010)

X-ray betatron radiation is produced by oscillations of electrons in the intense focusing field of a laser-plasma accelerator. These hard x-rays show promise for use in femtosecond-scale time-resolved radiography of ultrafast processes. However, the spectral characteristics of betatron radiation have only been inferred from filter pack measurements. In order to achieve higher resolution spectral information about the betatron emission, we used an x-ray charge-coupled device to record the spectrum of betatron radiation, with a full width at half maximum resolution of 225 eV. In addition, we have recorded simultaneous electron and x-ray spectra along with x-ray images that allow for a determination of the betatron emission source size, as well as differences in the x-ray spectra as a function of the energy spectrum of accelerated electrons. © *2010 American Institute of Physics.* [doi:10.1063/1.3479118]

I. INTRODUCTION

Laser driven plasma-based accelerators have the potential to become compact and cost efficient alternatives to conventional linear accelerators (linacs). In such accelerators, a femtosecond laser pulse drives a plasma wave whose space charge field accelerates electrons from the plasma.[1] Accelerating gradients on the order of GV/m have been measured in laser-plasma accelerators (LPA) which are three orders of magnitude higher than in linacs.[2–5] Recent experiments have demonstrated the production of monoenergetic (few percent energy spread), high energy (hundreds of MeV), and high charge (hundreds of picocoulombs) electron bunches from a self-modulated LPA that used a preformed plasma density channel.[4,5]

Although the use of LPAs as replacements for high-energy physics accelerators will require further development, several applications of LPA can currently be realized. One such application is the generation and use of femtosecond x-ray pulses produced by the transverse (or betatron) oscillations of electrons in a focusing field of the plasma wake as they propagate through the plasma. For example, betatron radiation can be used to make femtosecond-scale time-resolved radiography of ultrafast processes such as plasma heating and material melting, as well as being a test bed for developing diagnostics of laser-plasma acceleration.

There have been several experiments on high peak-power laser facilities in which the nature (divergence and total x-ray flux) of the betatron radiation has been observed.[6,7] These measurements have validated theoretical calculations[8] that predict approximately 10^8 photons within a divergence of approximately 30 mrad for tens of MeV electron bunches with a nanocoulomb of charge. Here we present a measurement that highlights a new experimental technique enabling us to record high-resolution x-ray spectral information of betatron radiation. Furthermore, our measurement is able to discern changes of the betatron emission x-ray spectrum with differing laser parameters and to simultaneously image the laser-plasma interaction region while obtaining an energy resolved spectrum of both the x-rays and electrons.

II. EXPERIMENT AND RESULTS

In the experiment, a pulse from Berkeley's LOASIS Ti:sapphire laser was focused above a gas-jet nozzle oriented transversely to the beam line (see Fig. 1).[9] The peak power was 10 TW [0.45 J in 45 fs full width at half maximum (FWHM)] and was focused onto a 7.5 μm FWHM spot. The plasma density profile had a peak density of 3×10^{19} cm^{-3}. The charge per bunch and electron beam spatial profile were measured using an integrating current transformer (ICT) and a phosphor screen coupled to an optical charge-coupled device (CCD), located 50 and 75 cm away from the nozzle of the gas jet, respectively. The response of the phosphor screen to number of counts on the optical CCD versus deposited charge was calibrated against the ICT.[10] The energy distribution was obtained using a single shot magnetic spectrometer that deflected the electrons onto a phosphor screen and was imaged onto a CCD. The observable energy range spans

[a)]Contributed paper, published as part of the Proceedings of the 18th Topical Conference on High-Temperature Plasma Diagnostics, Wildwood, New Jersey, May 2010.

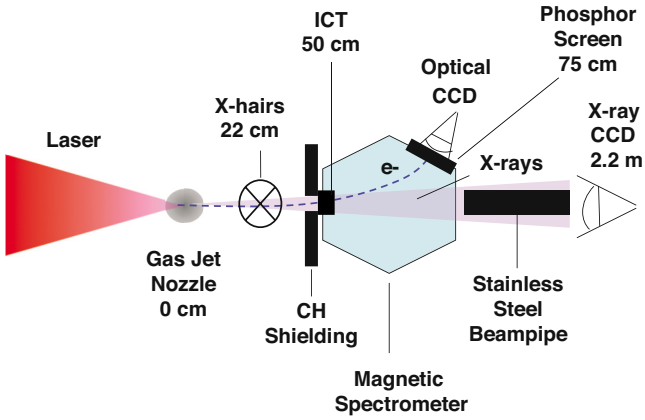

FIG. 1. (Color online) Schematic of the experimental setup. Distances of various elements used in the measurement are indicated. All distance values are referenced from the gas-jet nozzle which is labeled as 0 cm.

10–90 MeV. The accelerator was operated in the self-modulated regime, and as such, shows a broad energy spread with some quasimonoenergetic features. The electron beam spectra of an average of 200 single shots for two different accelerator parameter sets (labeled "High" and "Low") are shown in Fig. 2. Both electron spectra and x-ray data were taken simultaneously.

In order to image and obtain a spectrum of the x-ray emission, a 1024×256 pixel back-illuminated CCD camera with 26 μm square pixels and a 40 μm deep depletion region was placed 220 cm from the laser/gas-jet interaction region. The operation of the CCD required a higher vacuum than provided by the laser-plasma interaction chamber and, thus, a thin window was installed which kept the vacuum in the laser interaction chamber separate from that of the CCD. The thin window consisted of approximately 0.1 μm of aluminum, 14 μm of polycarbonate, and 18 μm of Kapton. In addition there was a 25 μm Be window in front of the CCD chip. The CCD imaged the interaction region and was aligned to the laser beam axis using a low-power beam from the laser system. Two sizes (12.5 μm diameter and 50 μm diameter) of gold plated tungsten fiber wires (California Wire Co.) were fabricated to form crosshairs and were optically aligned to the beam-CCD axis. The cross hairs were placed 22 cm from the laser/gas-jet interaction region (see Fig. 1).

The CCD camera was placed inside of a lead brick enclosure that helped to reduce stray γ-ray and x-ray background from hitting the camera. This background typically

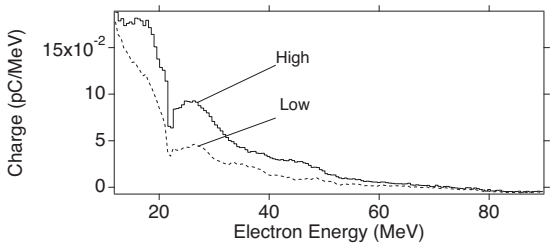

FIG. 2. Electron energy spectra averaged over 200 shots. (Solid) High: the set of accelerator parameters that produced the highest intensity betatron radiation. (Dashed) Low: set of accelerator parameters that produced weak betatron radiation. The dip that occurs around 22 MeV is an artifact of the analysis

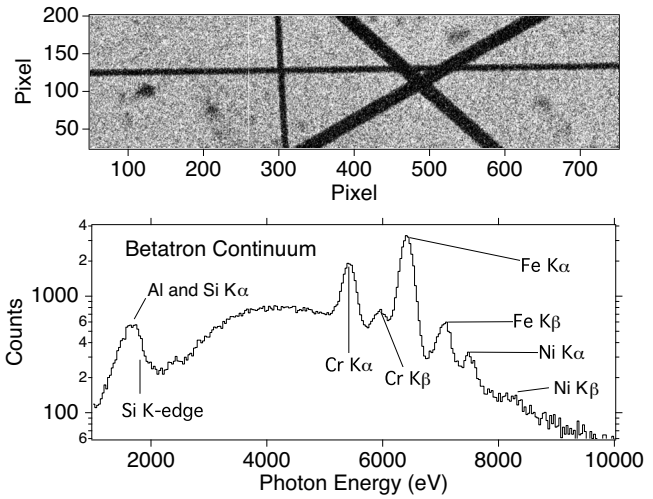

FIG. 3. Above: Image from the CCD obtained by accumulating 200 shots while operating the LPA at the High setting (see Fig. 2). The image shows the shadowgraph of the 12.5 and 50 μm thick wires. Below: Addition of the raw spectra from the 200 shots used to create the above image. The *K*-shell fluorescence lines from the stainless steel are identified as are the $K\alpha$ lines from Si and Al and the *K*-edge of Si. The betatron continuum is identified as the background in the spectrum.

results from the stopping of the tens of MeV electron beam in the magnetic spectrometer. The line of sight of the camera was restricted by a rectangular stainless steel pipe that was fitted to the size of the CCD chip ($\sim 25 \times 7$ mm^2). In order to reduce the on-axis hard x-ray bremsstrahlung, the forward angles of the aluminum target chamber were lined with plastic (CH) to slow down and stop any low-energy electrons. Figures 3 and 4 show the spectra and images recorded with the CCD for two different pulse lengths of the laser beam. The electron energy spectrum labeled High in Fig. 2 is from the same data set that produced Fig. 3 and the spectrum Low in Fig. 2 is from the same data set that produced Fig. 4. The energy scale of the spectra were calibrated using the centroids of *K*-shell fluorescence lines (determined by fitting the

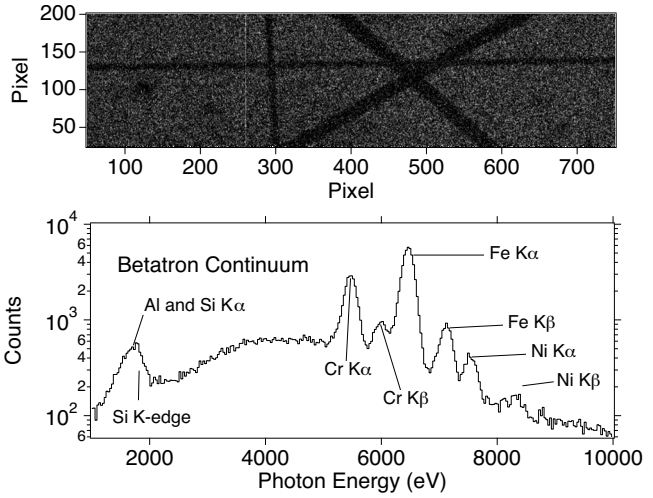

FIG. 4. Above: Image from the CCD obtained by accumulating 200 shots while operating the LPA at the Low setting (see Fig. 2). The image shows the shadowgraph of the 12.5 and 50 μm thick wires. Below: Addition of the raw spectra from the 200 shots used to create the above image. The same spectral features are identified as in Fig. 3.

lines to Gaussian fitting functions) from the stainless steel (Cr, Fe, and Ni) beam pipe downstream from the cross hairs. These lines were present in every spectrum. In addition, at the very low-energy range of the spectrum, there is a contribution from Al *K*-shell and Si *K*-shell fluorescence lines coming from the aluminized thin window and an effective CCD dead layer (estimated to be 1 μm thick).

In silicon CCD cameras, an electron is created for every 3.65 eV of energy from the absorbed x-ray; thus, the size of the signal from a pixel in a CCD is a direct measure of the x-ray energy. A histogram of the CCD image can then be used to generate a spectrum. If a large number of photons are recorded by the CCD in a single exposure frame then there is a risk that multiple photons are absorbed in a region that is close together and the accumulated charges combine to form a single event. Since we are operating in the regime where a large fraction of the CCD is illuminated, we use a routine that only histograms single pixel absorption events (SPAE). These SPAE are x-ray hits in which the charge from the absorption is contained in a single pixel that is well separated from other accumulated charge on the CCD. The FWHM resolution of our measurement was determined to be 225 eV.

III. DISCUSSION

Knowledge of the total x-ray flux emanating from a LPA is an important quantity and can be estimated from our experiment by looking at the occupancy (or amount of pixels that have accumulated charge) of the x-ray image in the CCD. By taking into account the size and placement of the CCD, the occupancy of ~50%, assuming a 30 mrad divergent x-ray beam (which is consistent with the uniform illumination of the CCD of x-rays seen in the experiment), and folding in the quantum efficiency of the CCD, we estimate that there are on the order of 10^8 photons/shot. This is in agreement with both theory and previous experiments.[6]

From the electron beam spectra shown in Fig. 2, the predicted spectrum of betatron emission peaks in the 0.5–1 keV energy range and has an exponential decay to higher photon energies. However, because of the thin window, the silicon *K*-edge, and both Al and Si $K\alpha$ lines the low-energy region of the spectrum is obscured by a large instrumental response correction. Nevertheless, a deconvolution of the instrumental response (with large uncertainties) from the spectra in Figs. 3 and 4 shows an exponentially decaying continuum. Further studies should measure betatron radiation well above the Si *K*-edge in order to remove uncertainties related to these low-energy features.

Comparison of the data from the two different accelerator settings shows both different x-ray and electron spectral characteristics. In Fig. 3, the intensity ratio of the iron and chromium fluorescence lines to the betatron continuum is much lower than in Fig. 4. This is attributed to a higher intensity of betatron emission which is indicative of a greater number of high-energy electrons (as high-energy electrons contribute to the betatron emission more than low-energy electrons). Indeed, the electron spectrum for the High data set shows a greater number of high-energy electrons. In addition, the hump centered around 4 keV in Fig. 3 is more pronounced and is a different shape than what is found in Fig. 4. We interpret this to be a change in the peak of the betatron emission as there is a higher number of photons at higher energies.

Since the CCD was able to directly image the interaction region, by measuring the sharpness of the shadow caused by the crosshairs, it is possible to estimate the size of the x-ray emission region.[11] As an upper bound, the source size must be smaller than the 12.5 μm size of the thinnest wire cross hair as its shadow can clearly be seen. A more accurate measurement using a lineout that is perpendicular to the edge (or "shadow of the wire surface") from Fig. 3 yields a shot-integrated source size of 6 ± 3 μm.

To the best of our knowledge, we have made the first measurement where an x-ray image, a high-resolution x-ray spectrum, and electron spectrum have been obtained simultaneously to characterize betatron radiation. The use of our SPAE algorithm for producing the x-ray spectra is robust and has yielded an extensive improvement in the spectral information of the emission over previous published results. Using this technique opens up future studies in which all of these processes can be studied in more detail, such as a focus on using narrow bandwidth monoenergetic electron beams of higher energy to selectively explore the parameter space in order to benchmark theoretical calculations.

ACKNOWLEDGMENTS

We would like to thank Don Syversrud, Zachary Eisentraut, and Nathan Ybarrolaza for expert technical support without whom this measurement would not have been possible. This work was supported in part by the U.S. DOE Office of Science Contract No. DE-AC02-05CH11231, by grants from the U.S. DOE NNSA NA-22, NSF Grant No. 0614001, and the Alliance Program of the Helmholtz Association (Grant No. HA216/EMMI).

[1] T. Tajima and J. M. Dawson, Phys. Rev. Lett. **43**, 267 (1979).
[2] W. P. Leemans, C. G. R. Geddes, J. Faure, *et al.*, Phys. Rev. Lett. **91**, 074802 (2003).
[3] C. G. R. Geddes, K. Nakamura, G. R. Plateau, *et al.*, Phys. Rev. Lett. **100**, 215004 (2008).
[4] S. P. D. Mangles, C. D. Murphy, Z. Najmudin, *et al.*, Nature (London) **431**, 535 (2004); C. G. R. Geddes *et al.*, *ibid.* **431**, 538 (2004); J. Faure *et al.*, *ibid.* **431**, 541 (2004).
[5] J. Osterhoff, A. Popp, Zs. Major, *et al.*, Phys. Rev. Lett. **101**, 085002 (2008).
[6] K. T. Phuoc, S. Corde, R. Shah, *et al.*, Phys. Rev. Lett. **97**, 225002 (2006).
[7] A. Rousse, K. T. Phuoc, R. Shah, *et al.*, Phys. Rev. Lett. **93**, 135005 (2004).
[8] E. Esarey, B. A. Shadwick, P. Catravas, *et al.*, Phys. Rev. E **65**, 056505 (2002); K. T. Phuoc, E. Esarey, V. Leurent, *et al.*, Phys. Plasmas **15**, 063102 (2008).
[9] The Lasers Optical Accelerator Systems Integrated Studies (LOASIS) is a core program within the Accelerator and Fusion Research Division of the Lawrence Berkeley National Laboratory. See http://loasis.lbl.gov.
[10] K. Nakamura, W. Wan, N. Ybarrolaza, *et al.*, Rev. Sci. Instrum. **79**, 053301 (2008).
[11] S. Kneip, S. R. Nagel, C. Bellei, *et al.*, Phys. Rev. Lett. **100**, 105006 (2008).